

ON THE POSSIBILITY OF SIMULTANEOUSLY MEASURING PROFILES OF THE KEY METEOROLOGICAL PARAMETERS

A.I. Grishin, G.G. Matvienko, O.V. Kharchenko, and T.A. Yarchuk

*Institute of Atmospheric Optics,
Siberian Branch of the Russian Academy of Sciences, Tomsk
Received July 15, 1994*

The potentiality of a lidar facility to measure profiles of the key meteorological parameters of the atmosphere by the differential absorption method for determining temperature and humidity by the correlation technique for measuring the wind velocity vector is investigated in this paper. The accuracy of the measurements carried out is estimated. Maximum ranges for the optical system are determined.

In remote determination of meteorological parameters of the atmosphere, the rate of extracting the needed information may be of particular importance. Therefore it is interesting to study the feasibility of simultaneous measurements of temperature and humidity profiles together with the vector of wind velocity using lidars.

A three-frequency method of differential absorption (MDA) for measuring temperature and humidity and a phase method for determining wind velocity were chosen as basic methods for their performance in the meteorological lidar. The possible use of a combined data array is the basis for the unified measurement technique.

Within the framework of the approach to solution of this problem we have carried out a numerical experiment on sounding the key meteorological parameters of the atmosphere with the MEL-01 lidar operating in a three-path optical arrangement of sounding.¹ The general configuration of the lidar is depicted in Fig. 1. It should be noted that each path is related to a particular wavelength. The radiation at $\lambda_1 = 725.7947$ nm and $\lambda_2 = 725.7378$ nm is emitted in the first and second directions, respectively. Both of these wavelengths correspond to the region of water vapor absorption. The radiation at $\lambda_3 = 725.7500$ nm emitted in the third direction corresponds to the atmospheric transmission window.

The determination of wind velocity under absorption along the sounding path results in additional damping of the optical signal which increases with the distance according to the exponential law. This, in turn, decreases the signal-to-noise ratio and hence reduces the sounding range. The calculations show that for the given lidar the limiting range of sounding, at which the variance of lidar return fluctuations is compared to that due to shot noises of the signal, is about 1 km for summer and 1.7 km for winter. The difference in characteristics is caused by different content of water vapor in the atmosphere in winter and summer.

To check the calculation, we constructed the wind profiles under the conditions of lidar return absorption. It should be noted that real lidar returns at wavelengths off the absorption lines were taken as the basis. Then these signals were corrected taking into account the absorption for summer conditions, and the wind velocity profile was reconstructed from them. The temporal series stored along the three paths from 128 vertical levels were digitally filtered to compensate for trends and to decrease the level of high-frequency components. Then the obtained data were subjected to Fourier transform based on a fast algorithm, whereupon the findings were multiplied in pairs. From the obtained complex products the correlation functions were found by the method of inverse fast Fourier transform. The

wind velocity profile was reconstructed from the shifts of their maxima.

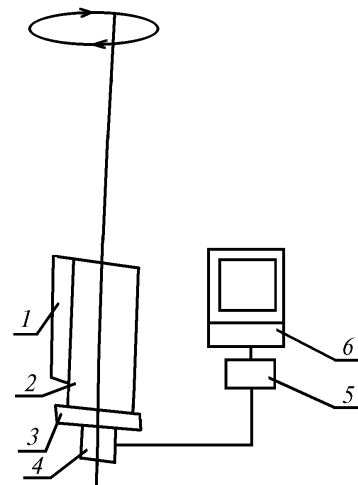


FIG. 1. Block-diagram of a three-path lidar MEL-01: 1) transmitter-laser ILTI-407; 2) receiver; 3) scanning unit; 4) photodetector unit; 5) analog-to-digital converter; and, 6) computer IBM PC AT.

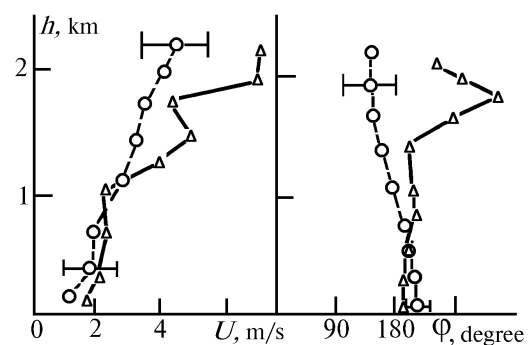


FIG. 2. The result of reconstructing the wind velocity profiles.

The result of reconstruction is presented in Fig. 2, where the solid lines show the wind velocity reconstructed from the initial data, and the dashed curves show that reconstructed from the corrected ones. The horizontal bars are a confidence intervals with the confidence coefficient of 0.95.

As seen from the figure, in the presence of absorption in the atmosphere the correct reconstruction of the wind velocity profile is possible up to 1–1.2 km altitude. Above these height the error becomes unacceptable. Thus, these results support the earlier conclusion about the maximum ranges of sounding of the wind velocity in the absorbing atmosphere.

In the numerical experiment on sounding the humidity and temperature profiles, we used the spectral parameters of the absorption lines from the GEISA Atlas,² the aerosol characteristics and meteorological parameters of the atmosphere from the McClatchey's model,³ and the altitude behavior of the scattering phase function from the model by Krekov and Rakhimov.⁴

The water vapor concentration $r(h)$ averaged over the altitude interval Dh can be found from the relation

$$\rho(h) = \alpha_1(h) / (K_1(h) - K_0(h)), \quad (1)$$

where

$$\alpha_1(h) = (1/2 \Delta h) \ln\{U_1(h)U_0(h + \Delta h) : [U_1(h + \Delta h)U_0(h)]\}; \quad (2)$$

$K_i(h)$ is the altitude dependence of the absorption coefficient at the wavelengths on ($i = 1$) and off ($i = 0$) the water vapor absorption line which is calculated from the *a priori* information about the distribution of thermodynamic parameters of the atmosphere and spectral structure of laser radiation; $U_1(h)$ and $U_1(h + \Delta h)$ are the lidar returns from the volumes sounded that are at the distances h and $h + \Delta h$ from the lidar. The temperature profile acquired using the tree–frequency method is reconstructed as

$$T(h) = T_0 A / (\ln C - \ln F(h)), \quad (3)$$

where

$$A = (E_1 - E_2) / (k T_0), \quad (4)$$

$$C = S_{01} \gamma_{02} / (S_{02} \gamma_{01}) \exp(A), \quad (5)$$

$$F(h) = \alpha_1(h) / \alpha_2(h); \quad (6)$$

E_j , S_{0j} , and γ_{0j} are the energy of the lower rotation–vibration level, intensity, and the halfwidth of the absorption line at temperature T_0 and pressure P_0 for the first and the second absorption line, $j = 1, 2$. The extinction coefficient $\alpha_2(h)$ is determined as in the case with $\alpha_1(h)$ (Eq. (2)).

To estimate the precision characteristics of the lidar, we calculated the errors in reconstructing the profiles T and r which are accounted for by, first, random errors in the lidar return record and, second, systematic errors in the lidar MDA. To take into account the random errors in the experiment, the noise was introduced into the lidar returns. In this case, the random number generator was used to provide a homogeneous distribution of a noise component with an amplitude which is equivalent to shot noise of a real lidar return. The meteorological parameters were reconstructed by averaging over 1024 pulses that corresponds to a real size of data arrays.

The increase of the temperature measurement error due to spatial separation of the points of information extraction was simulated by additional random temperature fluctuations of 0.1° introduced into the signal channels.

Depicted in Fig. 3. are the reconstructed and simulated temperature for mid–latitude winter and summer. As seen from the figure, the temperature reconstruction with the accuracy to 1° is possible in the lower layer of the atmosphere up to 1.5 km altitude. As expected, the error increases with altitude. The results of humidity profile reconstruction for mid–latitude winter and summer are depicted in Fig. 4. The error does not exceed 1% at distances to 1.8 km.

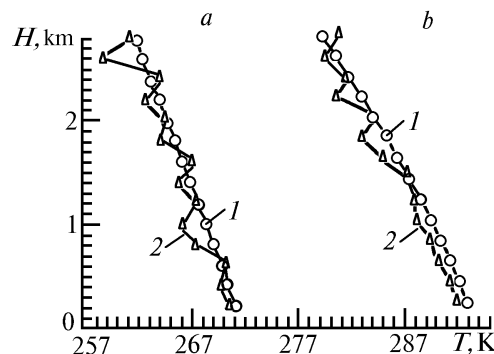


FIG. 3. The results of reconstructing the temperature profiles: reconstructed (1) and simulated (2) profiles for mid–latitude winter (a) and summer (b).

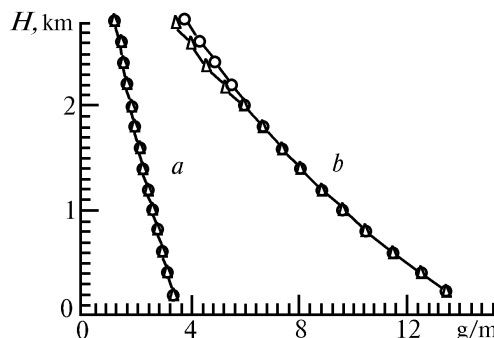


FIG. 4. The results of reconstructing the humidity profiles: simulated (triangles) and reconstructed (circles) profiles for mid–latitude winter (a) and summer (b).

TABLE I. Errors in reconstructing the temperature profiles.

$r, \text{ km}$	$\Delta v_e, \text{ cm}^{-1}$		
	0,01	0,03	0,05
0.200	0.8030	1.2340	2.0691
0.400	0.7724	1.2144	2.0701
0.600	0.8377	1.2929	2.1733
0.800	1.0182	1.4893	2.3997
1.000	1.0372	1.5216	2.4562
1.200	0.8651	1.3589	2.3095
1.400	0.8048	1.3102	2.2806
1.600	0.8806	1.4004	2.3956
1.800	1.1246	1.6624	2.6893
2.000	1.0911	1.6425	2.6939
2.200	0.7369	1.2953	2.8599
2.400	0.5671	1.1351	2.2177
2.600	0.6474	1.2307	2.3388
2.800	1.0894	1.6903	2.8358

In the second part of the numerical experiment, we considered systematic errors of the lidar MDA due to errors in preliminary calculation of the absorption coefficient

profiles which in real sounding schemes must be represented as effective values averaged over the emission spectrum (K_{eff}). Also considered was the effect of the laser radiation line width on K_{eff} used in reconstructing the profiles of meteorological parameters under study. The calculations were made for three values of the laser radiation line width $\Delta\nu_e = 0.01, 0.03, \text{ and } 0.05 \text{ cm}^{-1}$. The absolute error of the temperature profiles for different $\Delta\nu_e$ is given in the table. As seen from the table, the error is within 1.5° when $\delta\nu_e = 0.01 \text{ cm}^{-1}$, and it does not exceed 2° when $\Delta\nu_e = 0.05 \text{ cm}^{-1}$.

The numerical experiment revealed that the errors of reconstructing the temperature and humidity profiles have acceptable values.

In conclusion it should be noted that depending on the volume of the stored information this method provides a 25–50% increase in the measurement rate of meteorological

parameters of the atmosphere as compared to the separate sounding of the same parameters.

REFERENCES

1. G.G. Matvienko, Yu.F. Arshinov, A.I. Grishin, et al., in: *Proceedings of XI Symposium on Laser and Acoustic Sounding of the Atmosphere*, Tomsk, Institute of Atmospheric Optics (1993), pp. 130–136.
2. N. Hasson, A. Chedin, N.E. Scott, et al., *Annales Geophysical. Fasc. 2. Series A*, 185–190 (1986).
3. G.M. Krekov and R.F. Rakhimov, *Opto–Radar Model of Continental Aerosol* (Nauka, Novosibirsk, 1982), 198 pp.
4. R.A. McClatchey, R.W. Fenn, J.E.A. Selby, et al., "Optical properties of the atmosphere," Report AFCRL–71–0279, AFCRL (Bedford, 1971), 86 pp.